

# Simplified quantification method for *in vivo* SPECT imaging of the Vesicular Acetylcholine Transporter with 123I-IBVM

Joachim Mazère<sup>1,2,3\*</sup>, Willy Mayo<sup>1,2</sup>, Guillaume Pariscoat<sup>1,2</sup>, Jürgen Schulz<sup>1,2</sup>,  
Michele Allard<sup>1,2,3,4</sup>, Philippe Fernandez<sup>1,2,3</sup>, and Frédéric Lamare<sup>1,2,3</sup>.

1. Univ. Bordeaux, INCIA, UMR 5287, F-33000 Bordeaux, France.
2. CNRS, INCIA, UMR 5287, F-33000 Bordeaux, France.
3. Service de médecine nucléaire, CHU de Bordeaux
4. EPHE, Paris, France

\*Address for correspondance:

Dr Joachim Mazère, PharmD, PhD  
Institut des Neurosciences Cognitives et Intégratives d'Aquitaine  
Université de Bordeaux  
146 rue Léo Saignat  
33076 Bordeaux cedex, France  
Tel: +33 557656838  
Fax: +33 557656839  
Email: joachim.mazere@chu-bordeaux.fr

Financial support: This study was supported by Eisai Pharmaceuticals.

Total word count = 5361

## ABSTRACT

<sup>123</sup>I-iodobenzovesamicol (<sup>123</sup>I-IBVM) is a Single Photon Emission Computed Tomography (SPECT) selective radioligand for the vesicular acetylcholine transporter (VACHT), used to assess the integrity of cholinergic pathways in various neurological disorders. The current noninvasive method for quantitative analysis of <sup>123</sup>I-IBVM, based on a reference tissue modeling (MRTM2), requires repeated scans for several hours, limiting its application in clinical trials. The objective is to validate a simplified acquisition method based on a single <sup>123</sup>I-IBVM static scan preserving the quantification accuracy. Three acquisition times were tested comparatively to a kinetic analysis using MRTM2.

**Methods:** Six healthy volunteers underwent a dynamic SPECT acquisition comprising of 14 frames over 28 h and a magnetic resonance imaging (MRI) scan. MR images were automatically segmented, providing the volumes of 19 regions of interest (ROI). SPECT dataset were co-registered with MR images and regional time-activity curves were derived. For each ROI, a complete MRTM2 pharmacokinetic analysis, using the cerebellar hemispheres as reference region, led to the calculation of an <sup>123</sup>I-IBVM to VACHT binding parameter, the nondisplaceable binding potential ( $BP_{ND-MRTM2}$ ). A simplified analysis was also performed at  $t = 5$  h, 8 h and 28 h after injection, providing simplified  $BP_{ND}$ , given as  $BP_{ND-t} = C_{ROI} - C_{cerebellar\ hemispheres} / C_{cerebellar\ hemispheres}$ , with  $C =$  averaged radioactive concentration. **Results:** No significant difference was found between  $BP_{ND-5h}$ ,  $BP_{ND-8h}$  and  $BP_{ND-MRTM2}$  in all extra-striatal regions explored.  $BP_{ND-28h}$  were significantly higher than  $BP_{ND-5h}$ ,  $BP_{ND-8h}$  and  $BP_{ND-MRTM2}$  in 9 out of the 18 regions explored ( $p < 0.05$ ).  $BP_{ND-5h}$ ,  $BP_{ND-8h}$  and  $BP_{ND-28h}$  were significantly correlated

with  $BP_{ND-MRTM2}$  ( $p < 0.05$ ;  $\rho = 0.99, 0.98$  and  $0.92$  respectively). In the striatum,  $BP_{ND-28h}$  were significantly higher than  $BP_{ND-5h}$  and  $BP_{ND-8h}$ .  $BP_{ND-5h}$  differed significantly from  $BP_{ND-MRTM2}$  ( $p < 0.05$ ), with  $BP_{ND-5h}$  being 43.6% lower. **Conclusion:** In the extra-striatal regions, a single scan acquisition at  $t = 5$  h or  $t = 8$  h after injection provides quantitative results similar to a pharmacokinetic analysis. However, with the highest correlation and accuracy,  $t = 5$  h is the most suitable time to perform an accurate  $^{123}I$ -IBVM quantification. In the striatum, none of the three times has led to an accurate quantification.

**Key words:**  $^{123}I$ -IBVM; SPECT; VACHT; neurological disorders; single scan acquisition

## INTRODUCTION

Many recent studies have revealed the involvement of cholinergic impairments in neurological disorders leading to growing interest in *in vivo* imaging of cholinergic networks (1-3). 123I-iodobenzovesamicol (123I-IBVM) is a highly selective Single-Photon Emission Computed Tomography (SPECT) radioligand for imaging of the Vesicular Acetylcholine Transporter (VACHT), an *in vivo* pre-synaptic marker of the cholinergic neurons reflecting the integrity of the brain cholinergic pathways. Indeed, 123I-IBVM imaging demonstrated impaired cholinergic systems in various neurodegenerative diseases (4-7).

The current noninvasive method for quantification of 123I-IBVM SPECT data, based on the pharmacokinetic Multilinear Reference Tissue Model 2 (MRTM2) (8,9), allows the calculation of an 123I-IBVM to VACHT binding ratio, the nondisplaceable binding potential ( $BP_{ND}$ ). Even if the occipital cortex was classically used as reference region (9), the use of the cerebellum was also recently proposed (10) and particularly the cerebellar hemispheres (11). 123I-IBVM quantification with MRTM2 was successful in providing a better understanding of pathophysiology in neurological disorders involving cholinergic impairment (5,6). However, it requires repeated scans for several hours, limiting its application in large-scale clinical trials. Alternative methods exist to derive kinetic parameters from the analysis of the activity distribution at equilibrium, when the target-tracer association and dissociation rates are equal (12,13). In a previous study, we have shown that a consistent  $BP_{ND}$  calculation was possible using a single scan acquisition performed at  $t = 6$  h after injection (9). Indeed, a significant correlation was found with

the complete kinetic MRTM2, increasing with time and suggesting to extend the acquisitions beyond 6 h (9), possibly until 24 h after injection as proposed by Kuhl et al. (14). However, this simplified quantification method was performed only in the striatum, a region with a very high level of <sup>123</sup>I-IBVM binding, whereas cholinergic pathway dysfunctions involve other areas with very low levels of <sup>123</sup>I-IBVM binding.

In order to find out the optimal trade-off between accuracy and simplicity for <sup>123</sup>I-IBVM quantification throughout cholinergic pathways, we propose to assess the validity of a single SPECT scan acquisition method with <sup>123</sup>I-IBVM across the whole brain, by testing various single scan times of 5 h, 8 h and 28 h after injection. The proposed method will be compared with the kinetic MRTM2 method with dynamic imaging data acquired until 28 h after injection. In regard of the choice of the reference region, the similarity between the occipital cortex and the cerebellar hemispheres was assessed.

## **MATERIALS AND METHODS**

### **Subjects**

The participants consisted of 6 healthy volunteers (age =  $66.8 \pm 1.5$  years) without neuropsychiatric disorder based on a screening interview by an experienced senior neuropsychologist.

The study was initiated after protocol approval by the Institutional Human Ethics Committee (registration number 2002/01) and radioactive drug approval by the National Health Product Safety Agency. Before providing written consent, all participants were presented with the basic design of the study and were informed that they could

withdraw from the investigation at any time.

## **Radiochemistry**

<sup>123</sup>I-IBVM was prepared and controlled as previously described (7). Briefly, after radio-iodination, <sup>123</sup>I-IBVM was purified by High Pressure Liquid Chromatography and Sep-Pack<sup>®</sup> C18 classic cartridge (Waters; Milford, Mass) and filtered, leading to 10 ml of sterile solution of <sup>123</sup>I-IBVM. Prior to injection, the solution was assessed to be pyrogen-free using the Endosafe-PTS portable test system<sup>®</sup> (Charles River Laboratories, Wilmington, MA).

## **Scanning Protocol**

*Anatomic MR imaging.* For anatomical colocalization with the SPECT data, subjects underwent a three-dimensional T1 Magnetic resonance (MR) imaging sequence (repetition time (TR)/echo time (TE), 7.1/3.5 ms; 8 degrees flip angle; field of view, 256 × 256mm to cover the whole brain yielding 228 slices (1mm slice thickness; 1mm<sup>3</sup> isotropic voxel size) using a 1.5-T MR imaging system (Philips, Best, The Netherlands).

*SPECT-CT imaging.* SPECT imaging was performed on a SPECT/CT SYMBIA T2 camera (Siemens; Erlangen, Germany) equipped with low energy thin section collimators. Participants were orally given 400mg of potassium perchlorate 30 minutes before and 24 h after imaging. After a mean intravenous injection of  $235.1 \pm 41.9$  MBq of <sup>123</sup>I-IBVM, the dynamic SPECT images were acquired over 28 h at six different

times: five frames of 6 minutes starting at injection time, two 15 minutes frames at 2 h, 3 h, 5 h and 8 h after injection and one final 15 minutes frame at 28 h after injection (64 projections with a matrix of 64 X 64 over 360 degrees). Between each of the first five acquisitions, the participants were allowed to rest outside of the gantry.

SPECT images were reconstructed on a 64×64 matrix by using a flash three-dimensional iterative reconstruction (four iterations, eight subsets) and a voxel size of 6.8×6.8×6.8 mm<sup>3</sup>. Attenuation correction was performed based on the CT image, as well as decay correction and normalization for frame duration. All the frames were rigidly registered together and with the CT image, to ensure the patient's brain was in the exact same position in all the images during the creation of the dynamic SPECT dataset.

### **SPECT Data processing**

*SPECT Data Registration to MR Images.* For each subject, the participants' CT and MR images were rigidly coregistered and the transformation parameters were subsequently applied to the SPECT dataset, providing a four-dimensional dynamic SPECT image registered to the MR image.

*Partial Volume Effect Correction of the Dynamic SPECT Dataset.* The MR-coregistered SPECT image was corrected for partial volume effect (PVE) using the

Muller-Gartner MR based method (15), implemented in the PMOD® software (version 3.3, PMOD Technologies, Zurich, Switzerland; <http://www.pmod.com>). For each subject, the MR was automatically segmented into gray matter, white matter and cerebrospinal fluid probability maps and the partial volume correction procedure subsequently proceeded, correcting the SPECT data for gray matter spill-out and white matter spill-in.

### **Time Activity Curves Calculation**

For each participant, the MR-registered and PVE-corrected dynamic SPECT data was used for derivation of regional time-activity curves. For each subject, the MR image was automatically segmented using the Freesurfer® software (16), providing the volumes and labels of 19 gray matter regions of interest (ROI), including various cortical and subcortical structures: orbitofrontal cortex, dorsal- and ventro-lateral cortices, motor and pre-motor cortices, anterior prefrontal cortex, primary visual cortex, inferior and middle occipital cortices, superior occipital cortex, superior parietal cortex, inferior parietal cortex, temporal cortex, anterior cingulate cortex, posterior ventral cingulate cortex, posterior dorsal cingulate cortex, hippocampus, amygdalo-hippocampal complex, thalamus, striatum, cerebellar vermis and cerebellar hemispheres. The PMOD® software was used to subsequently apply this gray matter template to each frame of the registered and PVE-corrected dynamic SPECT data to obtain average-decay corrected regional activities, which were plotted against time to derive regional time-activity curves.

## Pharmacokinetic Model

*Theory of Model Based Analysis.* Compartment modeling describes brain uptake and binding of radiotracer. The ordinary differential equations describing the two-tissue compartment models are

$$dC_{ND}(t) / dt = K_1 C_p(t) - (k_2+k_3)C_{ND}(t) + k_4C_S(t) \quad (1)$$

$$dC_S(t) / dt = k_3C_{ND}(t) - k_4C_S(t)$$

$$C_T(t) = C_{ND}(t) + C_S(t)$$

where  $C_p$  is the radiotracer concentration in plasma,  $C_T$  is the regional time activity curve of the radiotracer in the tissue of interest,  $C_S$  is the specifically bound radiotracer concentration in tissue,  $C_{ND}$  (non displaceable) is the free and non specifically bound radiotracer concentration in tissue. The rate constants  $K_1$  (mL/g per minute) and  $k_2$  (per minute) describe the influx and efflux of the radiotracer through the blood-brain barrier respectively and the rate constants  $k_3$  (per minute) and  $k_4$  (per minute) describe the tracer transfer between the non displaceable ( $C_{ND}$ ) and the specific binding ( $C_S$ ) compartment (9).

In a reference region, a region devoid of receptor sites,  $k_3 = 0$  and the model reduces to a one-tissue compartment described by the equation

$$dC'_{ND}(t) / dt = K'_1 C_p(t) - k'_2 C'_{ND}(t) \quad (2)$$

where  $C'_{ND}$  is the radiotracer concentration in the reference region and the rate constants  $K'_1$  and  $k'_2$  describe the influx and efflux of the radiotracer to and from the reference region (9).

*Quantification of 123I-IBVM SPECT Data.* In a previous study (9), pharmacokinetic modeling using multilinear reference tissue model 2 (MRTM2) (8) was shown to best correlate with invasive blood-sampling analysis (14), and was therefore considered as the reference method for noninvasive quantification of 123I-IBVM data. A two-step approach used with MRTM2, combining calculation of the reference region-to-plasma  $k'_2$  and multilinear regression analysis (9) led, for each ROI, to the calculation of the nondisplaceable binding potential ( $BP_{ND}$ ) value, a parameter whose value is proportional to the density of receptor sites, in this case, VACHT binding sites.

In the present study, we tested two 123I-IBVM quantification methods. First, we applied the MRTM2 method and calculated 123I-IBVM to VACHT  $BP_{ND}$  values for each participant and each ROI, by using the cerebellar hemispheres as reference region. We also applied a simplified analysis to calculate  $BP_{ND}$  values, based on a single scan acquisition at times of  $t = 5$  h, 8 h and 28 h after injection. Theoretically, a simplified analysis is valid at peak equilibrium, when the specific binding is maximum, corresponding to  $dC_S(t) / dt = 0$  (9,12,13). Assuming that  $C_{ND} = C'_{ND}$ , from equation (1), we have:

$$BP_{ND} = k_3 / k_4 = C_S / C'_{ND} = (C_T - C'_{ND}) / C'_{ND}$$

Consequently, in the proposed simplified analysis,  $BP_{ND}$  values were calculated for each participant, each ROI and each selected single scan time, as  $BP_{ND-t} = (C_{ROI} - C_{\text{cerebellar hemispheres}}) / C_{\text{cerebellar hemispheres}}$ , where  $C$  is the averaged radioactive concentration measured at the selected single scan time.

## **Statistical Analysis**

In each ROI, the Friedman repeated measures analysis of variance by ranks was used to assess differences between  $BP_{ND}$  values obtained with the four following methods: MRTM2, single scan acquired at either  $t = 5$  h,  $t = 8$  h or  $t = 28$  h after injection. Post-hoc paired comparisons were achieved with the Dunn's test. Correlations between  $BP_{ND}$  values calculated with a single scan acquisition and  $BP_{ND}$  values calculated with the MRTM2 method were assessed using Spearman correlations. Statistical analyses were performed using SPSS software version 22. (IBM SPSS Statistics for Windows, Armonk, NY: IBM Corp.) and STATISTICA<sup>®</sup> software version 9 (Statsoft, Tulsa, OK). A  $p$  value  $<0.05$  was considered statistically significant.

## **RESULTS**

### **Brain SPECT Images and Time Activity Curves**

For a representative subject, Figure 1 A shows images obtained at the acquisition times of  $t = 0$  h, 5 h, 8 h and 28 h post-injection. Immediately after injection, a typical image of cerebral blood flow with diffuse presence of the tracer is visible whereas a differential binding of  $^{123}\text{I}$ -IBVM appears over time, predominant in the striatum. Figure 1 B represents the time activity curves averaged over the population in some brain regions. The uptake is found to peak within the first 30 minutes, a characteristic phenomenon of flow-mediated tracer delivery in the brain. Two hours after injection, a sharp contrast between regions with high and low cholinergic

innervation is found, with the highest uptake in the striatum and the lowest in the cerebellar hemispheres, chosen as the reference region. This contrast is strengthened over time, by the fact that the tracer binding decreases in regions with moderate to low cholinergic innervation (thalamus, parahippocampal complex, vermis, cortical regions, cerebellar hemispheres) and remains stable in the striatum up to 28 h after injection. The mean striatal specific binding, calculated as the difference [striatum - cerebellar hemispheres] (dotted curve in the figure), reaches a maximum value at  $t = 8$  h after injection, held up until 28 h.

### **Reference region assessment**

Mean time activity curves obtained in the cerebellar hemispheres, the cerebellar vermis and the superior occipital cortex are visible in Figure 1 B. For a better visual assessment, Figure 2 shows curves obtained between  $t = 2$ h and  $t = 28$ h after injection, for the same regions of interest.  $^{123}\text{I}$ -IBVM concentrations were found to be higher in the vermis than in the cerebellar hemispheres. In the latter region,  $^{123}\text{I}$ -IBVM concentrations were found to be of similar magnitude than in the superior occipital cortex.

### **Quantitative Analyses in the Extra-Striatal Regions of Interest**

Results of  $\text{BP}_{\text{ND}}$  obtained for the extra-striatal regions from MRTM2 kinetic analysis and simplified analyses performed at  $t = 5$  h, 8 h and 28 h after injection are

presented in Figure 3 and Table 1. A Friedman repeated measures analysis of variance between the  $BP_{ND\ 5h}$ ,  $BP_{ND\ 8h}$ ,  $BP_{ND\ 28h}$  and  $BP_{ND\ MRTM2}$  values showed a significant difference in 9 out of the 17 explored regions ( $p < 0.05$ ). Post-hoc paired comparisons with the Dunn's test revealed that  $BP_{ND\ 28h}$  were significantly higher than  $BP_{ND\ 5h}$  and  $BP_{ND\ 8h}$  in 5 out of the 17 explored regions ( $p < 0.05$ ) and than  $BP_{ND\ 5h}$  in 2 out of the 17 explored regions ( $p \leq 0.01$ ). Post-hoc paired comparisons with the Dunn's test also revealed that  $BP_{ND\ 28h}$  were significantly higher than  $BP_{ND\ 5h}$  and  $BP_{ND\ MRTM2}$  in the hippocampus ( $p < 0.05$ ) and than  $BP_{ND\ 8h}$  in the dorsal and ventrolateral cortices ( $p < 0.05$ ).

A correlation study was performed between  $BP_{ND}$  evaluated with MRTM2 and  $BP_{ND}$  evaluated with the simplified analyses performed at  $t = 5\ h$ ,  $8\ h$  and  $28\ h$  after injection respectively (Figure 4). A significant correlation was found for all three methods:  $\rho = 0.99$ ,  $p < 0.05$ ;  $\rho = 0.98$ ,  $p < 0.05$ ; and  $\rho = 0.92$ ,  $p < 0.05$ , respectively.

### **Quantitative Analyses in the Striatum**

Results of  $BP_{ND}$  obtained in the striatum using the MRTM2 kinetic analysis and simplified analyses performed at  $t = 5\ h$ ,  $8\ h$  and  $28\ h$  after injection are presented in Table 2. A Friedman repeated measures analysis of variance between the  $BP_{ND\ 5h}$ ,  $BP_{ND\ 8h}$ ,  $BP_{ND\ 28h}$  and  $BP_{ND\ MRTM2}$  values showed a significant difference ( $p < 0.0001$ ). Post-hoc paired comparisons with the Dunn's test revealed that  $BP_{ND\ 5h}$  differed significantly from  $BP_{ND\ MRTM2}$  ( $p < 0.05$ ), with  $BP_{ND\ 5h}$  being 43.6% lower. Post-hoc paired

comparisons with the Dunn's test also showed that  $BP_{ND\ 28h}$  differed significantly from  $BP_{ND\ 5h}$  and  $BP_{ND\ 8h}$  ( $p < 0.05$ ).

A correlation study with the Spearman's test was performed between  $BP_{ND}$  evaluated with MRTM2 and  $BP_{ND}$  evaluated with the simplified analyses performed at  $t = 5\ h, 8\ h$  and  $28\ h$  respectively after injection (Figure 5). Highly significant correlations ( $\rho = 1$ ) were shown between  $BP_{ND\ 5h}$  and  $BP_{ND\ MRTM2}$  (A) and between  $BP_{ND\ 8h}$  and  $BP_{ND\ MRTM2}$ , and a significant, though less powerful ( $\rho = 0.94, p = 0.005$ ) correlation was found between  $BP_{ND\ 28h}$  and  $BP_{ND\ MRTM2}$  (C).

## DISCUSSION

Until now, the noninvasive method used to quantify  $^{123}I$ -IBVM consisted in a dynamic SPECT acquisition, comprising of 5 scans acquired until 7 h after injection, coupled with a post-processing MRTM2 kinetic analysis based on the use of the occipital cortex as reference region (9). In the present study, an alternative simplified  $^{123}I$ -IBVM method was evaluated based on the use of a single static acquisition. To this end, the SPECT dynamic acquisition was extended until 28 h after injection and several acquisition times were compared in order to determine the most suitable single static acquisition providing a simplified  $^{123}I$ -IBVM quantification without deteriorating the quantitative accuracy. The most important finding of the present study is that a single scan acquisition is able to provide a useful index for  $^{123}I$ -IBVM quantification. This result confirms the hypothesis stated previously that a simplified image acquisition protocol is

routinely usable in clinical practice to quantify 123I-IBVM (9).

In the first step of this methodological work, the choice of the occipital cortex as reference region to quantify 123I-IBVM to VAcHt BP<sub>ND</sub> was reconsidered. Indeed, in some neurodegenerative diseases, especially in dementia with Lewy bodies, characterised by occipital hypoperfusion and hypometabolism (17), tracer delivery in the occipital cortex may be altered compared with healthy subjects, leading to errors in the calculation of BP<sub>ND</sub> values in the remaining brain regions. Recently, the use of the cerebellum as reference region for quantification of 123I-IBVM SPECT data has been validated using an arterial input function (10). Furthermore, a recent study using a novel PET VAcHt radiotracer has shown in healthy subjects very similar levels of binding in the visual cortex and cerebellum as well as a differential cholinergic innervation within the cerebellum between the vermal region and the cerebellar hemispheres (11). This result challenges the statement that, from a cholinergic point of view, the occipital cortex is the most sparsely innervated region in the human brain. For this reason, in the present study, the cerebellar vermis was manually delineated and separated from the rest of the cerebellum. Consequently, 123I-IBVM uptakes were found to be higher in the vermis than in the cerebellar hemispheres and in the same magnitude when comparing the superior occipital cortex and the cerebellar hemispheres (Figure 1 B and 2). This result clearly demonstrates that 123I-IBVM is a suitable tracer to evidence a differential cholinergic innervation within the cerebellum. Moreover, with levels of tracer concentration comparable to those observed in the occipital cortex, the cerebellar hemispheres can reasonably be chosen as reference region for 123I-IBVM

quantification, especially in patients with dementia with Lewy bodies. In this study, the choice of the cerebellar hemispheres as reference region provided regional  $BP_{ND}$  values concordant with the known densities of cholinergic sites in the brain (18), high uptake levels being observed in the striatum, intermediate in the thalamus and cerebellar vermis and low in the cortical regions.

The finding that the specific binding curve of  $^{123}I$ -IBVM increases up to 6 h after injection in the striatum (Figure 1 B) is in line with our previous study in this region, suggesting a necessary extension of the SPECT acquisition beyond 6 h to reach the peak equilibrium time (9). The underestimation of  $BP_{ND\ 8h}$  and the overestimation of  $BP_{ND\ 28h}$  allow us to make the assumption that equilibrium in the striatum is reached at a time between  $t = 8$  h and  $t = 28$  h after injection, reflecting the very high expression of VAcHT in this region. On the opposite, brain regions with moderate to low cholinergic innervation, including the reference region of the cerebellar hemispheres, show rapid and constant tracer clearance from  $t = 2$  h until  $t = 28$  h after injection, demonstrating that maximum uptake in extra-striatal regions is reached earlier than in the striatum. These differences in tracer kinetics between regions with high and low cholinergic innervation are in line with our previous study, stating that the kinetics of the radiotracer concentration in the reference region and the free and non specifically bound radiotracer concentration in tissue were different (9).

As a consequence of such interregional variations of the  $^{123}I$ -IBVM radiotracer kinetics,  $BP_{ND\ 28h}$  is overestimated in several regions comparatively to  $BP_{ND\ 5h}$ ,  $BP_{ND\ 8h}$

and  $BP_{ND MRTM2}$  (Figure 3, Figure 4, Figure 5, Table 1 and Table 2). At first glance, such results argue against the possibility to perform an accurate quantification of  $^{123}I$ -IBVM at  $t = 28$  h after injection. However, two points are noteworthy concerning an  $^{123}I$ -IBVM single scan acquisition at  $t = 28$  h. First, a highly significant correlation was shown between  $BP_{ND 28h}$  and  $BP_{ND MRTM2}$  (Figure 4 D). Second, an acceptable — though less powerful — correlation ( $\rho = 0.86$ ,  $p < 0.05$ ; data not shown) was found between  $BP_{ND 28h}$  and  $k_3$  values calculated by Kuhl et al. with arterial blood sampling (14).

The overestimation of the  $BP_{ND}$  values, observed when a simplified analysis is performed at the late time of  $t = 28$  h after injection, is strongly attenuated when the analysis is conducted at earlier times, representing the main result of the present study. Indeed, no significant difference was found between  $BP_{ND 5h}$ ,  $BP_{ND 8h}$  and  $BP_{ND MRTM2}$  in all extra-striatal regions explored (Figure 3), providing evidence that a simplified and accurate analysis is feasible at early times. In Figure 4., the correlation study performed between  $BP_{ND MRTM2}$  and  $BP_{ND 5h}$ ,  $BP_{ND 8h}$  and  $BP_{ND 28h}$  shows the highest  $\rho$  value for a static analysis at  $t = 5$  h. Furthermore, based on the equations of the regression lines, the proposed simplified method provides reasonably accurate  $BP_{ND}$  values at the  $t = 5$  h time point (Figure 4 B) and overestimated  $BP_{ND}$  values at the  $t = 8$  h and 28 h time points (Figure 4 C and D), suggesting that overestimation increases with time. Thus, with the higher correlation and an acceptable accuracy, this result confirms that  $t = 5$  h after injection is the most suitable acquisition time to perform an accurate  $^{123}I$ -IBVM quantification in extra-striatal regions.

As far as the striatum is concerned, the significant correlations found for the three imaging times (Figure 5) demonstrate the feasibility of a simplified quantification. However, our results do not allow concluding on the most appropriate time to accurately quantify <sup>123</sup>I-IBVM. Indeed, an underestimation of -43.6% and -23.3% was observed at  $t = 5$  h and 8 h after injection respectively, whereas an overestimation of +36.1% was found at  $t = 28$  h after injection (Table 2). Slopes of the regression lines presented in Figure 5 confirm these results. These findings suggest that the most appropriate time to perform an accurate simplified quantification in the striatum is likely to be located few hours beyond  $t = 8$  h, in accordance with the specific binding curve in Figure 1B.

## CONCLUSION

In the extra-striatal regions, a single scan acquisition performed at  $t = 5$  h or  $t = 8$  h after injection provides quantitative results similar to a pharmacokinetic analysis, whereas acquisition at  $t = 28$  h tends to give higher results. Our study demonstrates that  $t = 5$  h is the most appropriate time to perform an accurate simplified quantification of <sup>123</sup>I-IBVM. Although less relevant from a practical point of view,  $t = 8$  h remains a valuable time, whereas  $t = 28$  h is less accurate. In the striatum, the richest region in cholinergic neurons, none of the three studied times has enabled an accurate quantification, probably because equilibrium is reached between 8h and 28 h after injection. Future work is needed to determine the appropriate time to acquire between 8 h and 28 h after injection.

## **ACKNOWLEDGMENTS**

The authors thank Eisai Pharmaceuticals Company (Tokyo, Japan) for financial support to M.A.

## REFERENCES

1. Hirano S, Shinotoh H, Shimada H, et al. Cholinergic imaging in corticobasal syndrome, progressive supranuclear palsy and frontotemporal dementia. *Brain*. 2010;133:2058-2068.
2. Gilman S, Koeppe RA, Nan B, et al. Cerebral cortical and subcortical cholinergic deficits in parkinsonian syndromes. *Neurology*. 2010;74:1416-1423.
3. Marcone A, Garibotto V, Moresco RM, et al. [(11)C]-MP4A PET cholinergic measurements in amnesic mild cognitive impairment, probable Alzheimer's disease, and dementia with Lewy bodies: a Bayesian method and voxel-based analysis. *J Alzheimers Dis*. 2012;31:387-399.
4. Kuhl DE, Minoshima S, Fessler JA, et al. In vivo mapping of cholinergic terminals in normal aging, Alzheimer's disease, and Parkinson's disease. *Ann Neurol*. 1996;40:399-410.
5. Mazere J, Meissner WG, Mayo W, et al. Progressive supranuclear palsy: in vivo SPECT imaging of presynaptic vesicular acetylcholine transporter with [123I]-Iodobenzovesamicol. *Radiology*. 2012;265:537-543.
6. Mazere J, Meissner WG, Sibon I, et al. 123I-IBVM SPECT imaging of cholinergic systems in multiple system atrophy: A specific alteration of the ponto-thalamic cholinergic pathways (Ch5–Ch6). *NeuroImage: Clin*. 2013;3:212-217.
7. Mazere J, Prunier C, Barret O, et al. In vivo SPECT imaging of vesicular acetylcholine transporter using [(123)I]-IBVM in early Alzheimer's disease. *Neuroimage*. 2008;40:280-288.
8. Ichise M, Liow JS, Lu JQ, et al. Linearized reference tissue parametric imaging methods: application to [11C]DASB positron emission tomography studies of the serotonin transporter in human brain. *J Cereb Blood Flow Metab*. 2003;23:1096-1112.
9. Barret O, Mazere J, Seibyl J, Allard M. Comparison of noninvasive quantification methods of in vivo vesicular acetylcholine transporter using 123I-IBVM SPECT imaging. *J Cereb Blood Flow Metab*. 2008;28:1624-1634.
10. Brasic JR, Bibat G, Kumar A, et al. Correlation of the vesicular acetylcholine transporter densities in the striata to the clinical abilities of women with Rett syndrome. *Synapse*. 2012;66:471-482.

11. Petrou M, Frey KA, Kilbourn MR, et al. In vivo imaging of human cholinergic nerve terminals with (-)-5-18F-Fluoroethoxybenzovesamicol: biodistribution, dosimetry, and tracer kinetic analyses. *J Nucl Med.* 2014;55:396-404.
12. Farde L, Eriksson L, Blomquist G, Halldin C. Kinetic analysis of central [11C]raclopride binding to D2-dopamine receptors studied by PET--a comparison to the equilibrium analysis. *J Cereb Blood Flow Metab.* 1989;9:696-708.
13. Ito H, Hietala J, Blomqvist G, Halldin C, Farde L. Comparison of the transient equilibrium and continuous infusion method for quantitative PET analysis of [11C]raclopride binding. *J Cereb Blood Flow Metab.* 1998;18:941-950.
14. Kuhl DE, Koeppe RA, Fessler JA, et al. In vivo mapping of cholinergic neurons in the human brain using SPECT and IBVM. *J Nucl Med.* 1994;35:405-410.
15. Muller-Gartner HW, Links JM, Prince JL, et al. Measurement of radiotracer concentration in brain gray matter using positron emission tomography: MRI-based correction for partial volume effects. *J Cereb Blood Flow Metab.* 1992;12:571-583.
16. Fischl B, Salat DH, Busa E, et al. Whole brain segmentation: automated labeling of neuroanatomical structures in the human brain. *Neuron.* 2002;33:341-355.
17. O'Brien JT, Colloby SJ, Pakrasi S, et al. Nicotinic alpha4beta2 receptor binding in dementia with Lewy bodies using 123I-5IA-85380 SPECT demonstrates a link between occipital changes and visual hallucinations. *Neuroimage.* 2008;40:1056-1063.
18. Mesulam MM, Hersh LB, Mash DC, Geula C. Differential cholinergic innervation within functional subdivisions of the human cerebral cortex: a choline acetyltransferase study. *J Comp Neurol.* 1992;318:316-328.

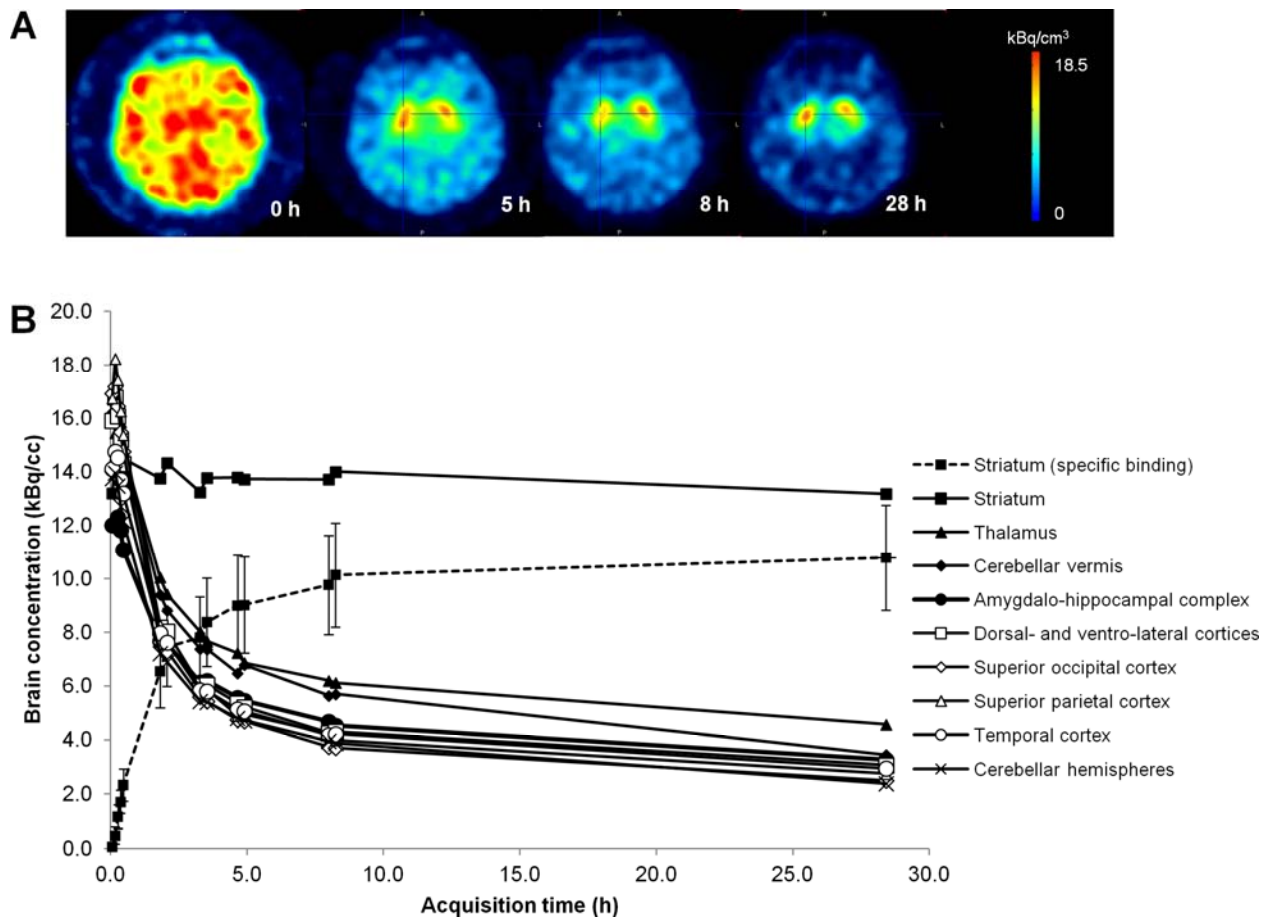


**FIGURE 1.**

Cross sectional SPECT images from one subject acquired at  $t = 0$  h, 5 h, 8 h and 28 h after injection (A) and characteristic tissue time-activity curves (the data are mean  $\pm$  standard error of the population) for some of the brain regions (solid lines) as well as of striatal-specific binding curve (dotted lines) (B).

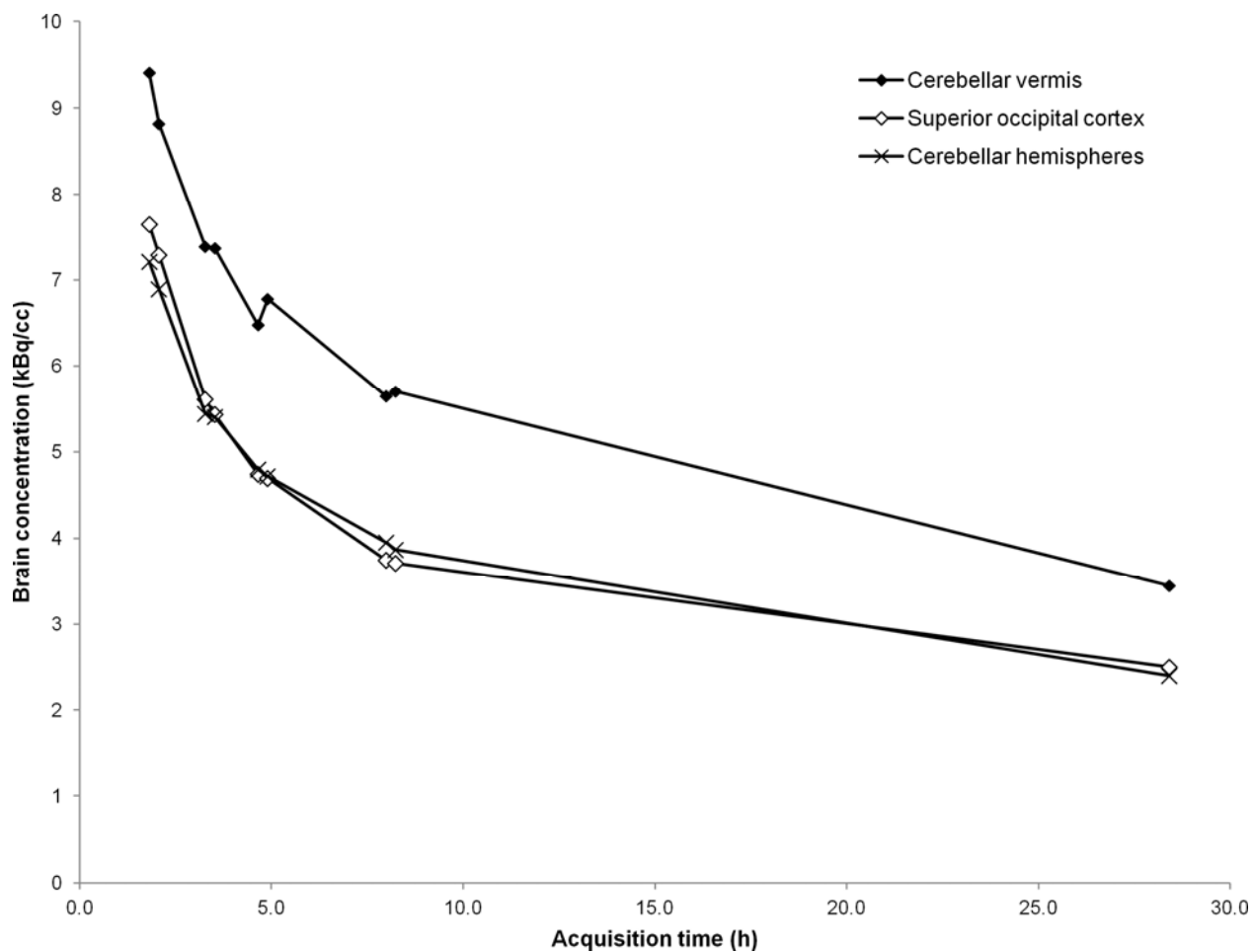


**FIGURE 2.**

Mean time activity curves obtained between  $t = 2$ h and 28 h after injection for the cerebellar vermis, the cerebellar hemispheres and the superior occipital cortex.

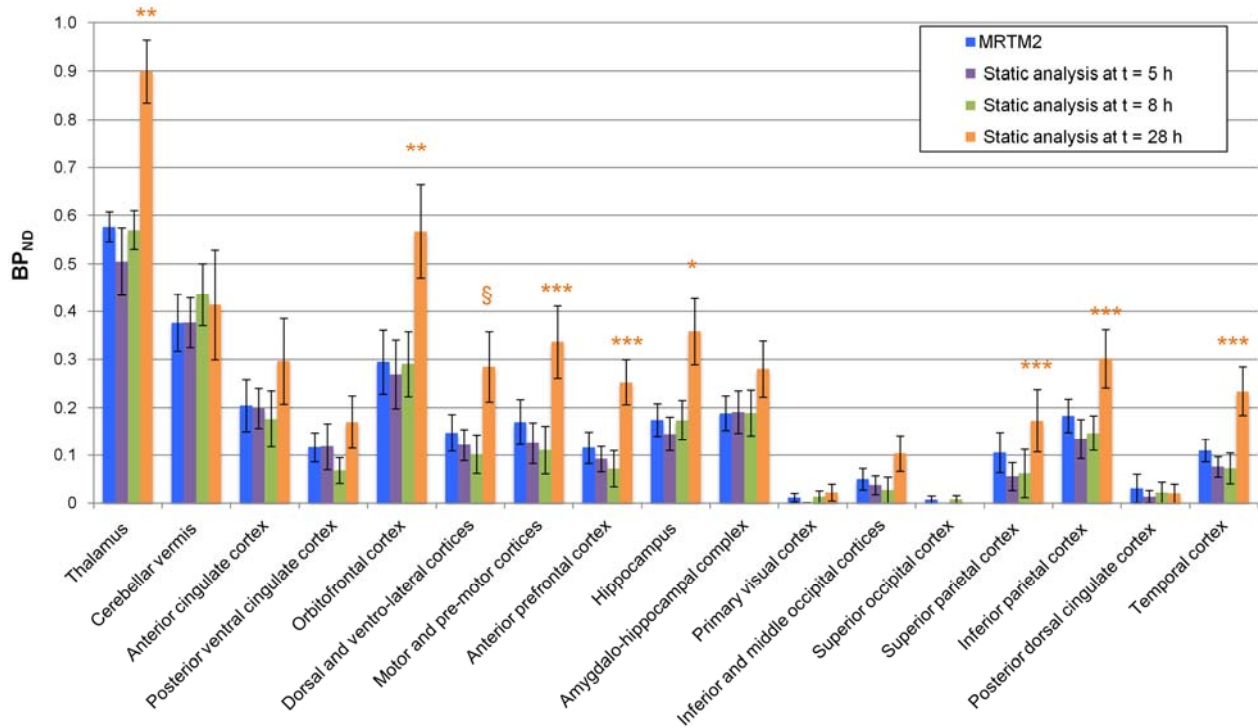


**FIGURE 3.**

Nondisplaceable binding potential ( $BP_{ND}$ ) values calculated in the extra-striatal regions of interest according to the method. The data are mean  $\pm$  standard error of the population. *MRTM2* = *Multilinear Reference Tissue Model 2*; (\*\*\*) = significant difference versus static analyses at  $t = 5$  h and  $t = 8$  h (Dunn,  $p < 0.05$ ); (\*\*) = significant difference versus  $t = 5$  h (Dunn,  $p \leq 0.01$ ); (\*) = significant difference versus MRTM2 and static analysis at  $t = 5$  h (Dunn,  $p < 0.05$ ); § = significant difference versus  $t = 8$  h (Dunn,  $p < 0.05$ ).

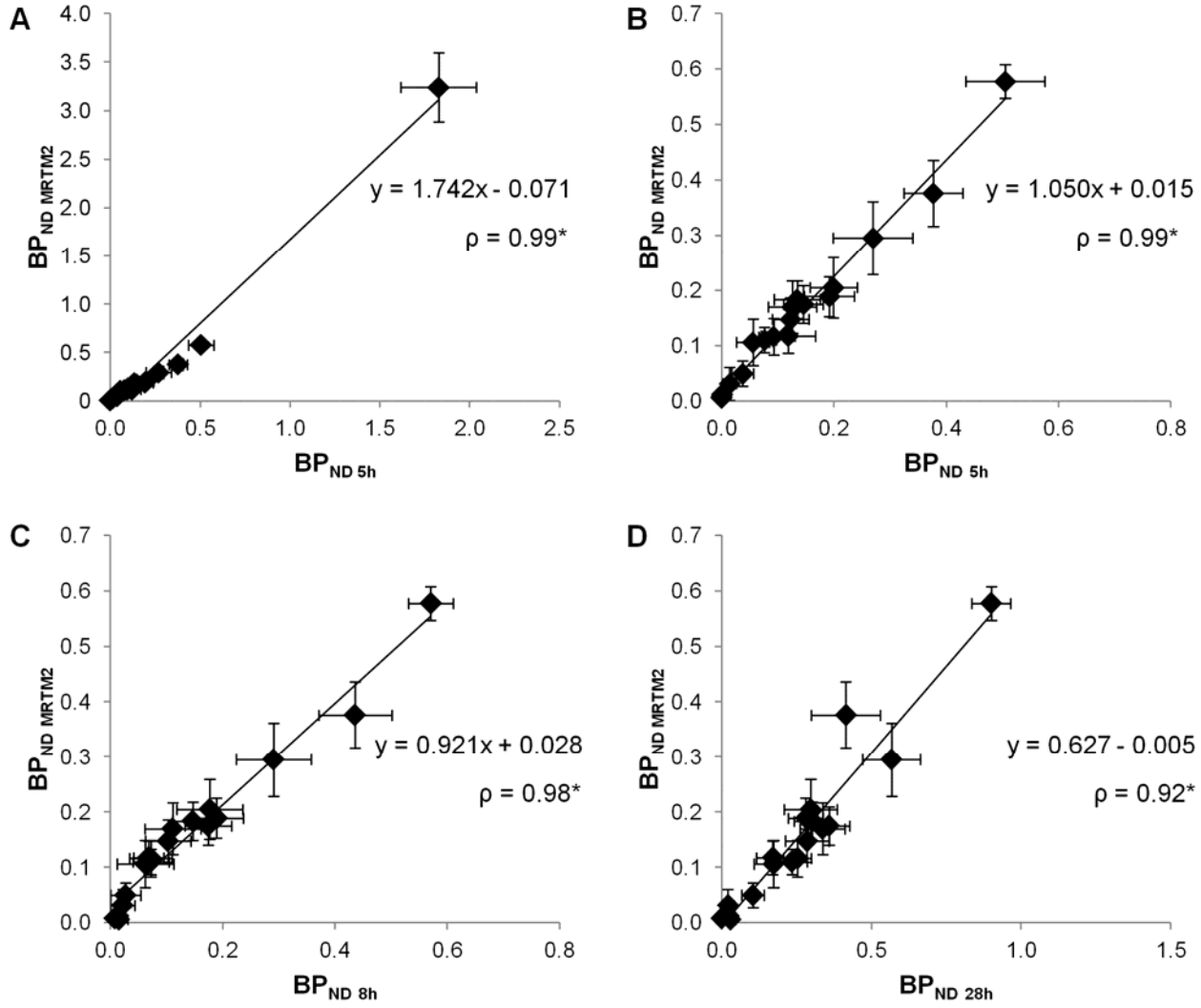


**FIGURE 4.**

Correlation between  $BP_{ND}$  values calculated using MRTM2 and those calculated using a static analysis at  $t = 5$  h (A and B),  $t = 8$  h (C) and  $t = 28$  h (D). As the striatum data point was very far from the others (A), the correlation coefficients were recalculated after exclusion of the data point (B, C and D). (\*) = *Statistically significant (Spearman,  $p < 0.05$ )*.

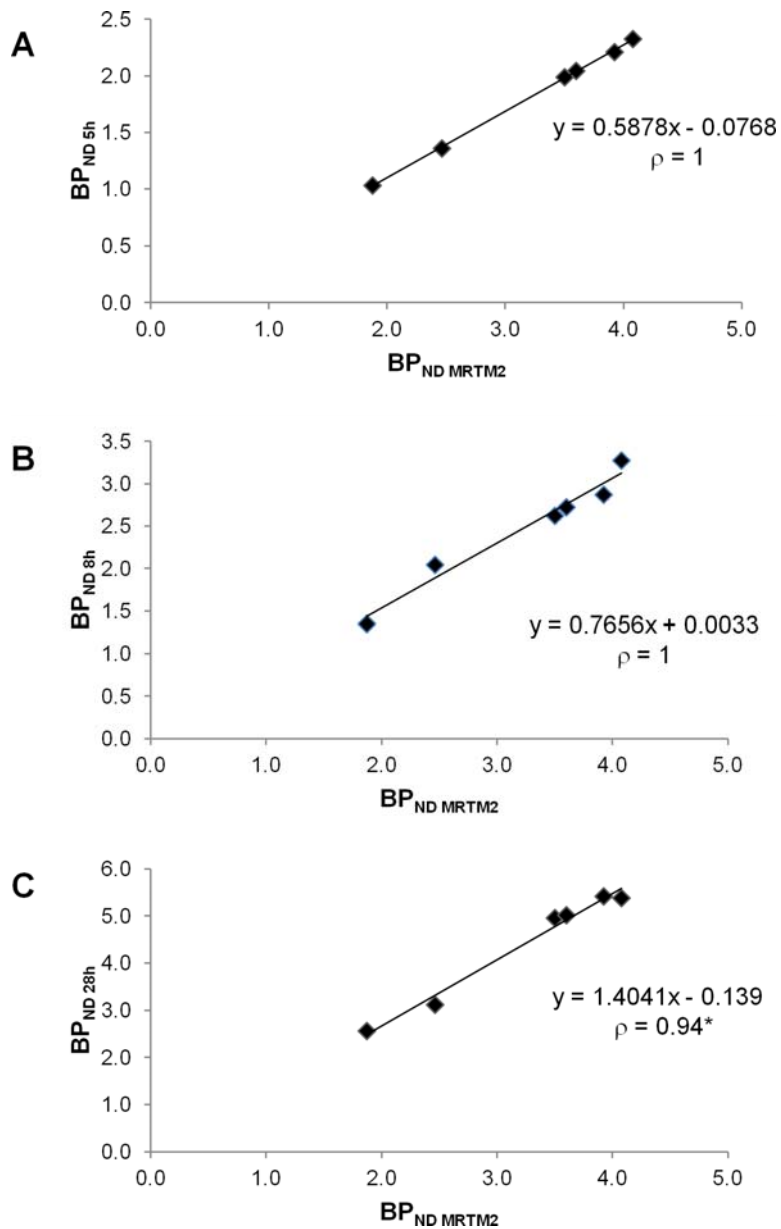


**FIGURE 5.**

Correlation study in the striatum between BP<sub>ND</sub> values calculated using MRTM2 and those calculated using a static analysis at t = 5 h (A), t = 8 h (B) and t = 28 h (C). (\* = Statistically significant (Spearman,  $p = 0.005$ )).

**TABLE 1**

BP<sub>ND</sub> values calculated in the extra-striatal regions of interest.

<b>Region of interest</b>	<b>Static analysis <i>t</i> = 5 hours</b>	<b>Static analysis <i>t</i> = 8 hours</b>	<b>Static analysis <i>t</i> = 28 hours</b>	<b>MRTM2</b>
Thalamus	0.51 ± 0.07	0.57 ± 0.04	0.90 ± 0.07	0.58 ± 0.03
Cerebellar vermis	0.38 ± 0.05	0.44 ± 0.07	0.41 ± 0.12	0.38 ± 0.06
Anterior cingulate cortex (BA 24, 32)	0.20 ± 0.04	0.18 ± 0.06	0.30 ± 0.09	0.21 ± 0.05
Posterior ventral cingulate cortex (BA 23)	0.12 ± 0.05	0.07 ± 0.03	0.17 ± 0.06	0.12 ± 0.03
Posterior dorsal cingulate cortex (BA 31)	0.01 ± 0.01	0.02 ± 0.02	0.02 ± 0.02	0.03 ± 0.03
Orbitofrontal cortex (BA 11, 12)	0.27 ± 0.07	0.29 ± 0.07	0.57 ± 0.10	0.30 ± 0.07
Dorsal and ventro-lateral cortices (BA 9, 44, 45, 46, 47)	0.12 ± 0.03	0.10 ± 0.04	0.29 ± 0.07	0.15 ± 0.04
Motor and pre-motor cortices (BA 4, 6, 8)	0.13 ± 0.04	0.11 ± 0.05	0.34 ± 0.08	0.17 ± 0.05
Anterior prefrontal cortex (BA 10)	0.09 ± 0.03	0.07 ± 0.04	0.25 ± 0.05	0.12 ± 0.03
Hippocampus	0.15 ± 0.04	0.17 ± 0.04	0.36 ± 0.07	0.18 ± 0.03
Amygdalo-hippocampal complex	0.19 ± 0.04	0.19 ± 0.05	0.28 ± 0.06	0.19 ± 0.04
Primary visual cortex (BA 17)	0.00 ± 0.00	0.01 ± 0.01	0.02 ± 0.02	0.01 ± 0.01
Middle and inferior occipital cortices (BA 18)	0.04 ± 0.02	0.03 ± 0.03	0.10 ± 0.04	0.05 ± 0.02
Superior occipital cortex (BA 19)	0.00 ± 0.00	0.01 ± 0.01	0.00 ± 0.00	0.01 ± 0.01
Superior parietal cortex (BA 1, 2, 3, 5, 7)	0.06 ± 0.03	0.06 ± 0.05	0.17 ± 0.07	0.11 ± 0.04
Inferior parietal cortex (BA 39, 40, 43)	0.13 ± 0.04	0.15 ± 0.04	0.30 ± 0.06	0.18 ± 0.04
Temporal cortex (BA 20, 21, 22, 41, 42)	0.08 ± 0.02	0.07 ± 0.03	0.23 ± 0.05	0.11 ± 0.02

The data are mean ± standard error of the population. *BA* = Brodmann Area numbers. *MRTM2* = Multilinear Reference Tissue Model 2.

**TABLE 2**BP<sub>ND</sub> values calculated in the striatum.

	<b>Static analysis t = 5 hours</b>	<b>Static analysis t = 8 hours</b>	<b>Static analysis t = 28 hours</b>	<b>MRTM2</b>
BP <sub>ND</sub>	1,83 ± 0,21*	2,48 ± 0,28**	4,41 ± 0,51****	3,24 ± 0,36***
Percentage change versus MRTM2	- 43,6 %	- 23,3 %	+ 36,1 %	-

The data are mean ± standard error of the population. (\*\*\*\*) *Significant difference versus 5 h and 8 h (Dunn, p<0.05)*; (\*\*\*) *Significant difference vs 5 h (Dunn, p<0.05)*; (\*\*) *Significant difference vs 28 h (Dunn, p<0.05)*; (\*) *Significant difference vs 28 h and MRTM2 (Dunn, p<0.05)*.